8186–8196 *Nucleic Acids Research, 2012, Vol. 40, No. 16* *Published online 6 June 2012*
doi:10.1093/nar/gks524

Contrasting enantioselective DNA preference: chiral helical macrocyclic lanthanide complex binding to DNA

Chuanqi Zhao[1], Jinsong Ren[1], Janusz Gregoliński[2], Jerzy Lisowski[2] and Xiaogang Qu[1,*]

[1]Division of Biological Inorganic Chemistry, State Key laboratory of Rare Earth Resources Utilization, Laboratory of Chemical Biology, Changchun Institute of Applied Chemistry, Graduate School of the Chine se Academy of Sciences, Chinese Academy of Sciences, Changchun, Jilin 130022, China and [2]Department of Chemistry, University of Wroclaw, Joliot-Curie 14, 50-383 Wroclaw, Poland

Received February 2, 2012; Revised April 29, 2012; Accepted May 11, 2012

ABSTRACT

There is great interest in design and synthesis of small molecules which selectively target specific genes to inhibit biological functions in which particular DNA structures participate. Among these studies, chiral recognition has been received much attention because more evidences have shown that conversions of the chirality and diverse conformations of DNA are involved in a series of important life events. Here, we report that a pair of chiral helical macrocyclic lanthanide (III) complexes, (*M*)-Yb[L_{ssssss}]$^{3+}$ and (*P*)-Yb[L_{RRRRRR}]$^{3+}$, can enantioselectively bind to B-form DNA and show remarkably contrasting effects on GC-rich and AT-rich DNA. Neither of them can influence non-B-form DNA, nor quadruplex DNA stability. Our results clearly show that P-enantiomer stabilizes both poly(dG-dC)$_2$ and poly(dA-dT)$_2$ while M-enantiomer stabilizes poly(dA-dT)$_2$, however, destabilizes poly(dG-dC)$_2$. To our knowledge, this is the best example of chiral metal compounds with such contrasting preference on GC- and AT-DNA. Ligand selectively stabilizing or destabilizing DNA can interfere with protein–DNA interactions and potentially affect many crucial biological processes, such as DNA replication, transcription and repair. As such, bearing these unique capabilities, the chiral compounds reported here may shed light on the design of novel enantiomers targeting specific DNA with both sequence and conformation preference.

INTRODUCTION

Chiral molecules have attracted considerable attention for rational drug design and for developing structural probes of DNA conformation, such as recognitions of left-handed Z-DNA (1–6) and G-quadruplex structures (7–10). There has been intense interest in design and synthesis of chiral metal complexes that target specific DNA sequences or DNA secondary structures to interfere with or control biological processes (11–16). Most of these metal complexes primarily centered around transition metal complexes, especially ruthenium polypyridyl complexes, which bear planar intercalating units that can insert into the base pairs of DNA double helix, serving as DNA intercalators (17–19). Besides these traditional ruthenium-based complexes, there is urgent need to design complex with novel molecular shape and exploit various central metals with unique characteristics for targeting polymorphic DNA structure and conformation (20,21). Lanthanide compounds, due to a unique $4f^n$ electronic configuration, have been widely used as probes in luminescent resonance energy transfer for bioassays and as reagents for diagnosis in magnetic resonance imaging (22,23). As chemical nucleases, lanthanide complexes have also shown a high efficiency to hydrolyze DNA and RNA without redox chemistry (24,25). There is great interest in the design and synthesis of lanthanide complexes which selectively target specific genes to inhibit biological functions in which particular DNA structures participate (26–28). However, there is no report to show a pair of chiral lanthanide complexes enantioselectively binding to DNA.

Ligand binding to DNA can disturb protein–DNA interactions and potentially affect many crucial biological processes (29,30). For instance, stabilizing DNA by drug molecules is an effective way to inhibit or disrupt DNA replication and transcription. When drug binding to duplex DNA, DNA unwinding would be disrupted because more energy was required to unzip the DNA helix, which directly influenced DNA replication and transcription (31). On the other hand, destabilization of the DNA helix induced by drugs is now known to strongly affect DNA repair process. It was reported that

*To whom correspondence should be addressed. Tel: +86 431 5262656; Fax: +86 431 85262656; Email: xqu@ciac.jl.cn

destabilization of double helix played an important role in the recognition of DNA lesions by repair proteins (32–34). Thus, modulating DNA stability using synthetic molecules is a promising strategy for realizing DNA-targeted anticancer and antiviral therapy. Herein, we report that a pair of chiral helical macrocyclic lanthanide (III) complexes which are different from conventional duplex DNA binders with planar motif, show contrasting enantioselectivity to duplex DNA. To the best of our knowledge, there is no report to show that any other chiral compounds bear these unique capabilities. Most of the reported chiral compounds show no or very weak selectivity on duplex DNA stability. For example, it has been reported that M-cylinder of a triple-helicate can target DNA major groove and induce DNA bending and intramolecular coiling more than does the P-cylinder. Nonetheless, both of the two enantiomers stabilize DNA with poor chiral selectivity (35). Tris(phenanthroline)ruthenium(II) enantiomers [$Ru(phen)_3^{2+}$] bound to right-handed DNA in two different binding modes: the Δ-isomer intercalates into the DNA helix and the Λ-isomer binds electrostatically along the groove, whereas both the isomers increased DNA melting temperature with a little quantitative difference between the two (36).

In the present work, we report that a pair of chiral helical macrocyclic lanthanide (III) complexes (M- and P-enantiomers) have remarkable enantioselectivity on B-form duplex DNA, however, neither of them can influence non-B-form duplex DNA or quadruplex DNA. P-enantiomer can stabilize both poly(dG-dC)$_2$ (GC-DNA) and poly(dA-dT)$_2$ (AT-DNA). Comparatively, M-enantiomer destabilizes GC-DNA, however, stabilizes AT-DNA. Quantitative binding data further indicate that P-enantiomer displays preferential binding to GC sequences while M-enantiomer prefers AT sequences. Stabilization or disruption of duplex DNA by drug binding can directly affect the unwinding of duplex, which is necessary for such vital processes as replication, transcription, recombination and repair (37). And as such, bearing these unique capabilities, the chiral complexes reported here may be potential drug candidates by inhibiting DNA replication and regulating biological functions that associated with duplex DNA. This is the first example that chiral complexes show contrasting enantioselectivity on GC- and AT-duplex DNA. Our work would shed light on the design of new chiral DNA-binding drugs with improved sequence-selectivity.

MATERIALS AND METHODS

DNA sequences

AT-DNA: 5′-ATATATATATATATATATATATATAT ATATATAT-3′
GC-DNA: 5′-GCGCGCGCGCGCGCGCGCGCGC GCGCGCGCGC-3′
Hairpin AT-DNA: 5′-HS-ATATATATATATCCCCAT ATATATATAT-3′
Hairpin GC-DNA: 5′-HS-GCGCGCGCGCGCTTTTGC GCGCGCGCGC-3′
AG_3: 5′-AGGGTTAGGGTTAGGGTTAGGG-3′
i-motif: 5′-CCCTAACCCTAACCCTAACCCT-3′
c-kit: 5′-AGGGAGGGCGCTGGGAGGAGGG-3′
c-myc: 5′-TGGGGAGGGTGGGGAGGGTGGGGAA GG-3′
A_{22}: 5′-AAAAAAAAAAAAAAAAAAAAAA-3′
T_{22}: 5′-TTTTTTTTTTTTTTTTTTTTTT-3′

DNA was synthesized by Shanghai Sangon Biological Engineering Technology & Services (Shanghai, China). Calf thymus DNA (ct-DNA) was obtained from Sigma, and purified and dialyzed as our previously described (38–40). The concentrations of DNA were determined by ultraviolet absorbance measurements. Chemicals were purchased from Sigma–Aldrich and used without further purification. All water used to prepare buffer solutions was obtained by using a Milli-Q water system. Ethidium bromide (EB), Hoechst 33258, 2-Mercaptoethanol (MCE, 99%) and methylene green (MG) and other reagents were purchased from Sigma and were used without further purification. All the experiments were carried out in Tris–HCl buffer (5 mM Tris, pH = 7.2) unless stated otherwise.

Synthesis of the complex

Enantiomerically pure (*M*)-$Yb[L_{SSSSSS}]^{3+}$ and (*P*)-$Yb[L_{RRRRRR}]^{3+}$ were synthesized and characterized as our previously described (41,42).

The gold substrates

The gold substrates (flat transparent glass chips were coated with a layer of 47 nm thick gold film) were purchased commercially from Thermo Electron Corp. (USA) and were carefully cleaned with piranha etch solution (4:1 concentrated H_2SO_4/30% H_2O_2) for 1 h at room temperature, and then thoroughly rinsed with ultrapure water and blown dry under a stream of N_2 before use.

Absorbance and UV melting

Absorbance measurements and melting experiments (38–40) were carried out on a Cary 300 UV/Vis spectrophotometer equipped with a Peltier temperature control accessory. All UV/Vis spectra were measured in 1.0-cm path-length cell with the same concentration of corresponding metal complex aqueous solution as the reference solution. Absorbance changes at either 260 or 295 nm versus temperature were collected at a heating rate of $0.5\,^{\circ}C\,min^{-1}$.

Thermodynamic studies

The enthalpy change, ΔH^0, was determined (38–40) from the temperature dependence of equilibrium association constant, where ΔH^0 was the slope of $\ln K_a$ versus $1/T$ plot according to the equation $\ln K_a = -(\Delta H^0/RT) + \Delta S^0/R$, where ΔS^0 was the entropy change that was calculated according to the *y*-axis intercept. The free energy change (ΔG^0_{25}) at 25°C was calculated from the standard Gibbs's equation, $\Delta G^0_{25} = \Delta H^0 - T\Delta S^0$.

Circular dichroism measurements

Circular dichroism (CD) spectra and CD melting experiments (43) were carried out on a JASCO J-810 spectropolarimeter equipped with a temperature controlled water bath. The optical chamber of CD spectrometer was deoxygenated with dry purified nitrogen (99.99%) for 45 min before use and kept the nitrogen atmosphere during experiments. Three scans were accumulated and automatically averaged. The various concentrations of M-enantiomer and P-enantiomer were scanned as a control and subtracted from the spectra of complex-DNA mixture to eliminate it. Binding constants of the enantiomers with DNA were measured by CD titrations, in which fixed concentrations of DNA titrated with increasing enantiomer concentrations. Changes in ellipticity at 275 nm of AT-DNA and changes in ellipticity at 280 nm of GC-DNA were plotted against enantiomer concentrations. Binding constants (K_a^{CD}) was estimated by fitting the data using a Fitall software (5).

Fourier transform-surface plasmon resonance experiments

Fourier transform-surface plasmon resonance (FT-SPR) experiments were performed on an SPR-100 FT-SPR spectrometer equipped with a Nicolet 6700 FT-IR main optical bench (Thermo Electron Corp., USA). The commercially purchased gold substrates (flat transparent glass chips were coated with a layer of 47 nm thick gold film) from Thermo Electron Corp. (USA) were used as the SPR sensor chips. Thiol-terminated DNA (100 µl) (10 µM in 5 mM Tris, 1.5 M NaCl, pH = 7.2) was injected into the flow cell and incubated for 12 h at room temperature. After being rinsed with Tris–HCl buffer (5 mM Tris, 1.5 M NaCl, pH = 7.2), 200 µl MCE (5 mM in Tris–HCl buffer) was injected and incubated for 1 h to block gold surface. Then, the MCE solution was removed by a thorough rinse with Tris–HCl buffer (5 mM Tris, pH = 7.2). Steady-state binding analysis was performed with injections of different complexes concentrations ranging from 0.1 to 3 µM over the immobilized DNA surface at a flow rate of 50 µl min^{-1} at 25°C. Complex solution flow was then replaced by running buffer (5 mM Tris, pH = 7.2) flow resulting in dissociation of the complex. The predicted maximum response in the steady-state region was determined from the DNA molecular weight, the amount of DNA on the flow cell, the complex molecular weight and the refractive index gradient ratio of the complex and DNA. The peak shift in steady-state regions at each concentration were converted to r (moles of compound bound per mole of DNA hairpin) as previously described. To obtain the affinity constants, the data generated were fitted with Kaleidagraph for non-linear least squares optimization of the binding parameters using the two-site binding model (the DNA immobilized on golden surface have two binding sites when bound with the enantiomers):

$$r = (K_1 C_{free} + 2K_1 K_2 C_{free}^2)/(1 + K_1 C_{free} + K_1 K_2 C_{free}^2)$$

where K_1 and K_2 are the macroscopic equilibrium binding constants; C_{free} is the free compound concentration at equilibrium and is actually the compound concentration in the flow solution herein.

Fluorescence measurements

Fluorescence measurements (40,43) were carried out on Jasco-FP-6500 spectrofluorometer (Jasco International Co. Ltd, Tokyo, Japan) using a quartz cell of 1 cm path length, at an excitation wavelength of 480 nm (EB) or 355 nm (Hoechst 33 258). Fluorescence emission spectra were monitored from 500 to 700 nm and from 370 to 620 nm, respectively. Slit widths for the excitation and emission were both set to 5 nm. All measurements were performed in Tris–HCl buffer (5 mM Tris, pH = 7.2) at 25°C.

RESULTS AND DISCUSSION

Enantioselectivity on GC- and AT-duplex DNA

The chiral helical macrocyclic lanthanide (III) complex used here is a pair of tricationic helical enantiomers consisting of a non-aazamacrocyclic amine wrapped in a helical fashion around the central Yb^{3+}. Enantiomerically pure (*M*)-Yb[L_{SSSSSS}]$^{3+}$ and (*P*)-Yb[L_{RRRRRR}]$^{3+}$ were synthesized as our previously described (41,42). UV melting and CD melting results show that both (*M*)-Yb[L_{SSSSSS}]$^{3+}$ and (*P*)-Yb[L_{RRRRRR}]$^{3+}$ are stable under our experimental conditions (Supplementary Figure S1).

UV melting assays were employed to study the influence of the two enantiomers on DNA stability (Supplementary Figure S2). Calf thymus DNA (ct-DNA, 42% GC and 58% AT), AT-DNA, GC-DNA were used and the variations of the melting temperature (ΔT_m, $\Delta T_m = T_m - T_m^0$) in the presence of the two enantiomers were shown in Figure 1 (38–40). Apparently, the chiral selectivity of (*M*)-Yb[L_{SSSSSS}]$^{3+}$ and (*P*)-Yb[L_{RRRRRR}]$^{3+}$ on stabilization of GC- or AT-duplex DNA is remarkable. For ct-DNA, its melting temperature (T_m) increased significantly with the increasing P-enantiomer and reached a platform at ~1:2 ratio of [P-enantiomer]: [ct-DNA] (The concentrations of duplex DNA were evaluated in base pairs) (Figure 1A). Compared to P-enantiomer, an interesting result was observed upon the addition of M-enantiomer. Initially, the stability of ct-DNA increased with increase of M-enantiomer. After that, however, DNA stability decreased with further increase of M-enantiomer. We presumed that this unusual behavior might result from the different affinity of M-enantiomer with different DNA sequences and M-enantiomer had different impacts on the stability of GC- or AT-duplex DNA. In this view, we investigated whether the two enantiomers displayed chiral selectivity toward different DNA. We next studied the effects of the P- and M-enantiomers on AT-DNA (Scheme 1A). Obviously, both P- and M-enantiomer can stabilize AT-DNA but P-enantiomer can stabilize AT-DNA much stronger than M-enantiomer (Figure 1B). The stronger stabilization by P-enantiomer should be due to its stronger AT binding affinity than M-enantiomer which will be quantitatively addressed in next binding studies. This preferential binding affinity of P-enantiomer toward AT-DNA could be attributable to

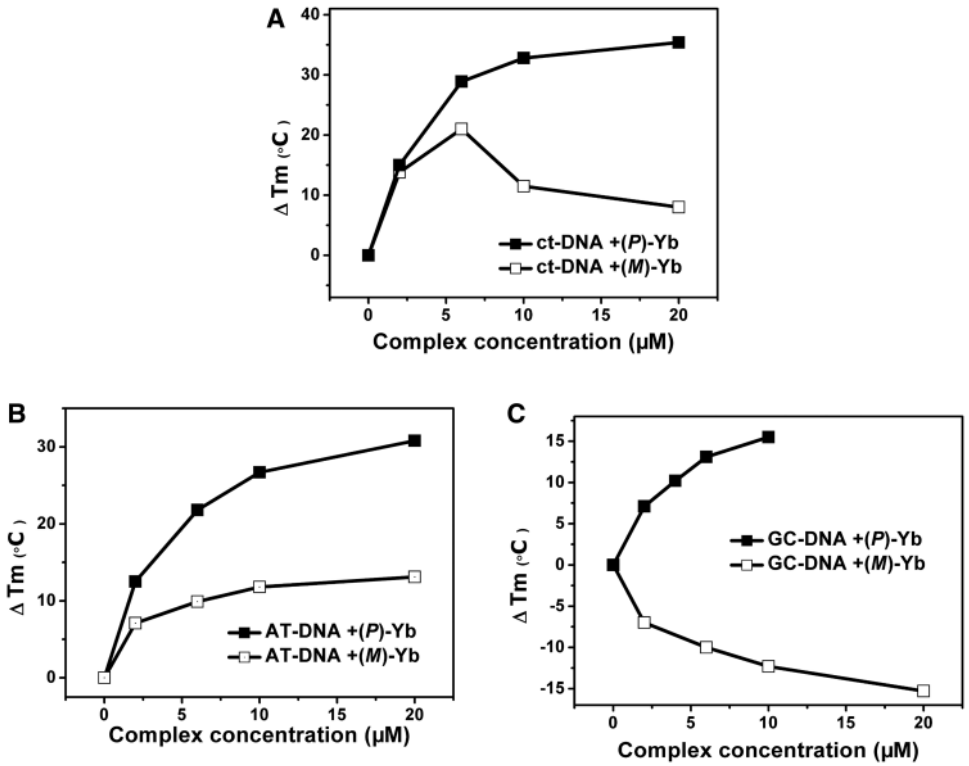

Figure 1. Variations of the melting temperature ΔT_m ($\Delta T_m = T_m - T_m^0$, T_m and T_m^0 represent the melting temperature of DNA in the presence or absence of complex) for complexes binding to ct-DNA (**A**), AT-DNA (**B**) and GC-DNA (**C**), respectively, as a function of concentration of (*P*)-Yb (solid square) and (*M*)-Yb (open square). DNA concentration was 20 μM in bp. T_m values were obtained from first-derivative plots of the thermal denaturation curves.

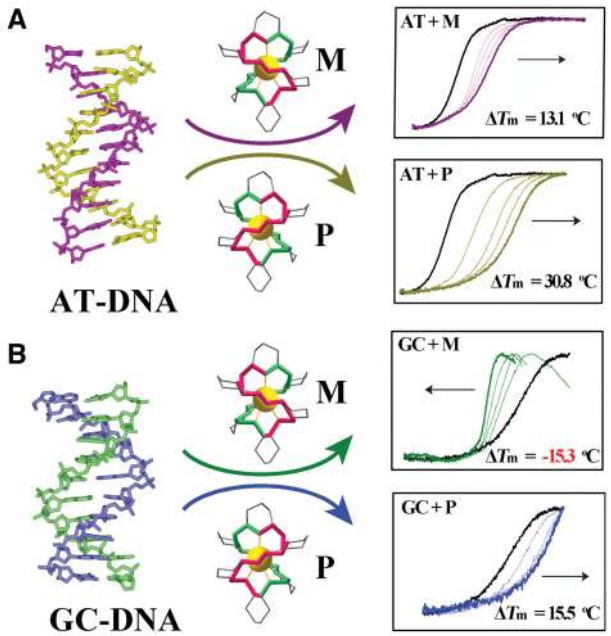

Scheme 1. (**A**) Chiral helical macrocyclic lanthanide (III) complexes (M- and P-enantiomer) can stabilize AT-DNA. P-enantiomer shows much stronger effect than M-enantiomer under the same conditions; (**B**) Contrasting enantioselectivity of M- and P-enantiomer on GC-DNA. M-enantiomer destabilize GC-DNA while P-enantiomer stabilize DNA under the same conditions. The structures of (*M*)-Yb$[L_{SSSSSS}]^{3+}$ and (*P*)-Yb$[L_{RRRRRR}]^{3+}$ complexes are based on crystallographic data reported previously (41,42).

the orientation of right-handed helical P-enantiomer, which may be more complementary with right-handed AT-DNA. This is consistent with previous report that interactions between helical molecules show a tendency for pairs of the same configuration of the helical molecules to form more stable complexes than pairs of enantiomeric helical molecules (44), indicating that right-handed P-enantiomer favors right-handed AT-DNA over left-handed M-enantiomer.

We next studied the effects of the enantiomers on GC-DNA (Scheme 1B). For P-enantiomer, similar to ct-DNA and AT-DNA, it can stabilize GC-DNA and increase the T_m by 15.5°C at 1:2 ratio of [P-enantiomer]/[DNA] (Figure 1C, solid points). In striking contrast, M-enantiomer decreases GC-DNA stability (Figure 1C, open points). The downward trend of negative ΔT_m value indicated that the stability of GC-DNA decreased rapidly in the presence of M-enantiomer. Clearly, M- and P-enantiomer show different effects on the stability of GC-DNA. This also satisfies the theoretical analysis that right-handed P-enantiomer favors right-handed GC-DNA, but left-handed M-enantiomer does not (44). It also should be noted that, in the presence of M-enantiomer, the GC-DNA UV absorption after melting transition decreased distinctly (Supplementary Figure S2D). This was assumed to be a consequence of the strong binding of the melted single-strand GC-DNA with M-enantiomer. To support this speculation, GC-DNA renaturation curves in the absence or presence of enantiomers were measured (Supplementary Figure S3). The results show that, when cooling down, the melted single-strand GC-DNA alone and in the presence of P-enantiomer can reform duplex, but can not in the presence of M-enantiomer. This assay indicates the strong binding of M-enantiomer with single-strand GC-DNA, which may be explained why M-enantiomer can decrease GC-DNA. Such a result is similar to our previous report that single-walled carbon nanotubes (SWNTs) selectively destabilized GC-DNA, and the decreased absorption after melting transition showed the strong interaction of single-strand GC-DNA with SWNTs (38). In addition, to further confirm that the two enantiomers selectively destabilize or stabilize GC-DNA, CD melting assays were carried out and the results were in good agreement with UV melting data (Supplementary Figure S4).

Thermodynamic studies on M- and P-enantiomer binding to DNA

For further understanding their interactions with DNA, thermodynamic parameters of DNA alone and in the presence of the two enantiomers were evaluated (Supplementary Figure S5) (39,40,43). The data were summarized in Table 1. AT-DNA stabilization by P-enantiomer was driven by a net favorable $\Delta\Delta G^0_{25} \sim -3.9\,\text{kcal mol}^{-1}$. The more favorable free energy was from more favorable entropy ($\Delta\Delta S^0 \sim 80.7\,\text{cal mol}^{-1}\,\text{K}^{-1}$) because its enthalpy was even less favorable than that of AT-DNA alone with a $\Delta\Delta H^0$ of $\sim 20.2\,\text{kcal mol}^{-1}$. These changes indicate that stabilization of the AT-DNA by P-enantiomer is due to favorable entropy contribution that exceeds an unfavorable enthalpy contribution (39,40,45,46). Similar results were also observed for AT-DNA stabilization by M-enantiomer, showing an enthalpy–entropy compensation (39,40,45). And also, GC-DNA stabilization by P-enantiomer is driven by net favorable free energy change, $\Delta\Delta G^0_{25} = -7.8\,\text{kcal mol}^{-1}$. Nonetheless, this more favorable free energy was from a more favorable enthalpy ($\Delta\Delta H^0$ of $\sim -36.6\,\text{kcal mol}^{-1}$) because its entropy was even less favorable than that of GC-DNA alone ($\Delta\Delta S^0 \sim -7.0\,\text{cal mol}^{-1}\,\text{K}^{-1}$). The results demonstrate that AT-DNA stabilization by P-enantiomer is entropy favorable, whereas the GC-DNA stabilization by P-enantiomer is enthalpy favorable. Destabilization of GC-DNA by M-enantiomer is due to an unfavorable entropic contribution that exceeds a favorable enthalpy contribution. These results indicate that P-enantiomer enthalpically stabilized GC-DNA and M-enantiomer entropically destabilized GC-DNA.

Table 1. Thermodynamic parameters of DNA alone and upon binding with (*M*)-Yb and (*P*)-Yb[a]

DNA	ΔH^0 (kcal mol^{-1})	ΔS^0 (cal mol^{-1} K^{-1})	ΔG^0_{25} (kcal mol^{-1})	T_m (°C)
AT-DNA	−73.9 ± 5.2	−236.8 ± 16.4	−3.2 ± 0.2	35.7
+M	−57.5 ± 6.9	−70.3 ± 21.1	−4.3 ± 0.5	47.5
+P	−53.7 ± 3.2	−156.1 ± 9.38	−7.1 ± 0.1	62.4
GC-DNA	−52.9 ± 3.7	−149.7 ± 10.3	−8.2 ± 0.5	74.4
+M	−76.4 ± 3.4	−233.4 ± 9.7	−6.7 ± 0.4	62.1
+P	−89.5 ± 17.0	−156.7 ± 35.5	−16.0 ± 3.0	89.9

[a]Experimental details were described in 'Materials and Methods' section.

Effects of M- and P-enantiomer binding on DNA conformation

CD studies were used to study DNA conformational alterations upon the two enantiomer binding. CD spectra of AT-DNA alone and in the presence of the two enantiomers are compared in Figure 2A and B, respectively, and CD backgrounds of the two enantiomers were subtracted. CD spectrum of AT-DNA alone consists of a positive band at 268 nm due to base stacking and a negative band at 247 nm due to helicity, which indicates that the AT-DNA adopted a typical B-form structure (27,39,40,47). As shown in Figure 2A, P-enantiomer binding to AT-DNA caused the positive band ~268 nm increased and blue shifted 5 nm and slightly decreased the negative band at 247 nm. This indicates that P-enantiomer binding slightly altered AT-DNA structure. For comparison, the parallel experiment was performed with M-enantiomer. Binding with M-enantiomer also brought about a decrease in negative band and a subtle blue shift of 2 nm in positive band, indicating that the influence of M-enantiomer binding was weaker than P-enantiomer binding. This was consistent with our UV melting results and will be further explained by quantitative binding studies described below. As for GC-DNA (Figure 2C and D), P-enantiomer binding caused slightly increase of the positive band at 280 nm and decrease of the negative

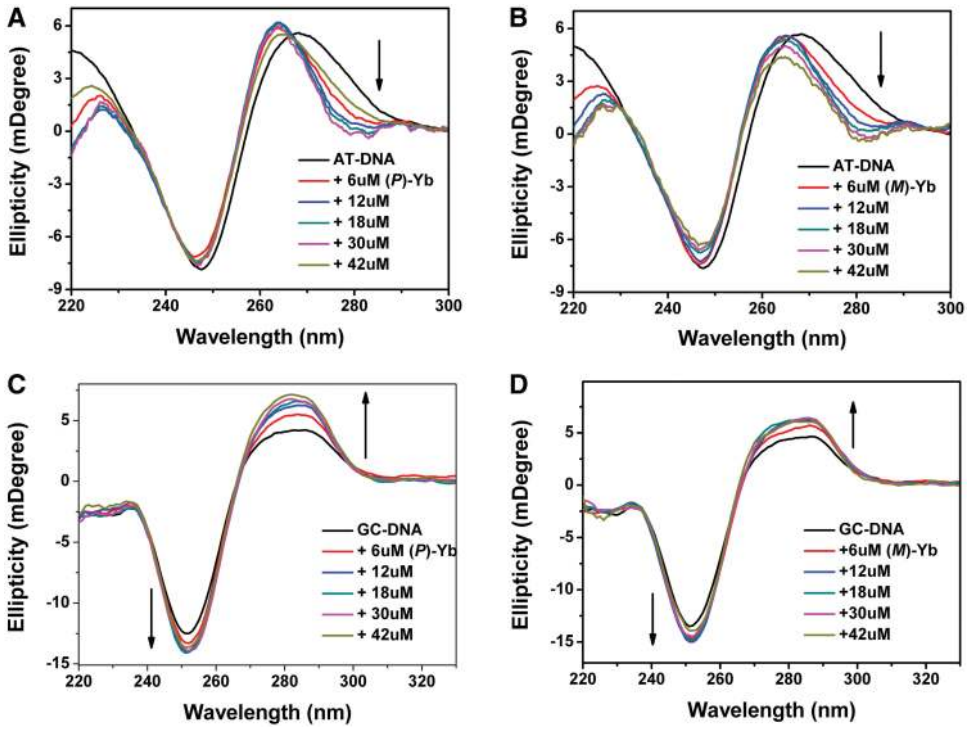

Figure 2. CD titrations of DNA with (*P*)-Yb or (*M*)-Yb in 5 mM Tris–HCl buffer (pH = 7.2) at 25°C. (**A**) AT-DNA was titrated with (*P*)-Yb; (**B**) AT-DNA was titrated with (*M*)-Yb; (**C**) GC-DNA was titrated with (*P*)-Yb; (**D**) GC-DNA was titrated with (*M*)-Yb. DNA concentration was 30 μM in bp and the complex concentrations were varied from 0 to 42 μM. The CD backgrounds of the two enantiomers were subtracted, respectively.

band at 252 nm, while M-enantiomer caused similar but weaker CD signal change, indicating its weak affinity compared to P-enantiomer. CD studies indicate that the two enantiomers binding to AT-DNA or GC-DNA do not strongly disrupt DNA structure. In consideration of the relative large size of the chiral complex, it suggests that the two enantiomers may bind to DNA possibly by groove binding, not by intercalation because DNA intercalators usually bring about significant DNA CD spectral changes (38–40,47). DNA CD intensity at 275 nm for AT-DNA or 280 nm for GC-DNA versus enantiomer concentration were used to estimate the binding stoichiometry of M- or P-enantiomer binding to AT-DNA and GC-DNA (Supplementary Figure S6), respectively. For AT-DNA, a break point was observed at ~4:1 binding ratio for both M-enantiomer and P-enantiomer, demonstrating that one enantiomer bound with 4 bp. As for GC-DNA, break point was observed at ratio of 3:1, showing that one enantiomer bound with 3 bp. This is consistent with the next competitive binding results, which are indicative that the two enantiomers are bound to DNA minor grooves. Previous studies have indicate that the minor groove of GC-DNA is relatively wider and shallower than that of AT-DNA, therefore, one enantiomer may cover 3 bp when bound to GC-DNA (38,39,48).

Determination of binding constants using SPR measurements

SPR technology has been used to investigate drug binding selectivity by using different DNA sequences. It can quantitatively determine binding constant and the cooperativity of drug–DNA interactions (49–51). In order to evaluate M- and P-enantiomer DNA binding affinity, we used SPR to study the two enantiomers binding to 28 bp AT- and GC-DNA as described in 'Materials and Methods' section. Sensorgrams for the enantiomers binding are depicted in Figure 3. By plotting the peak shift intensity as a function of the enantiomer concentration in the flow solution and using a two-site binding model (Figure 3E and F), we estimated the binding constants for P- and M-enantiomer binding to AT- and GC-DNA, respectively. The data are summarized in Table 2. The affinities for P- and M-enantiomer binding with GC-hairpins were determined to be 6.9×10^6 and $1.4 \times 10^6\,M^{-1}$, respectively, which represented 5-fold difference. This indicates that P-enantiomer binds stronger to GC-DNA than M-enantiomer. Furthermore, the interactions of the two enantiomers with DNA are not cooperative because two enantiomers bind 10-fold weaker to secondary non-specific binding sites (Table 2). The affinities for P- and M-enantiomer binding to AT-DNA were estimated to be 4.1×10^6 and $2.1 \times 10^6\,M^{-1}$, respectively, suggesting that P-enantiomer also binds stronger to AT-DNA than M-enantiomer. Binding constants were also measured by using CD titrations (Table 2). The binding constants obtained from this assay (K_a^{CD}) were lower than the value obtained from SPR analysis. It was reasonable because it has been reported that binding constants obtained using different methods might be significantly different (52). As expectedly, based on the K_a^{CD} values, the selectivity of the enantiomers binding to AT- and GC-DNA was in good agreement with the

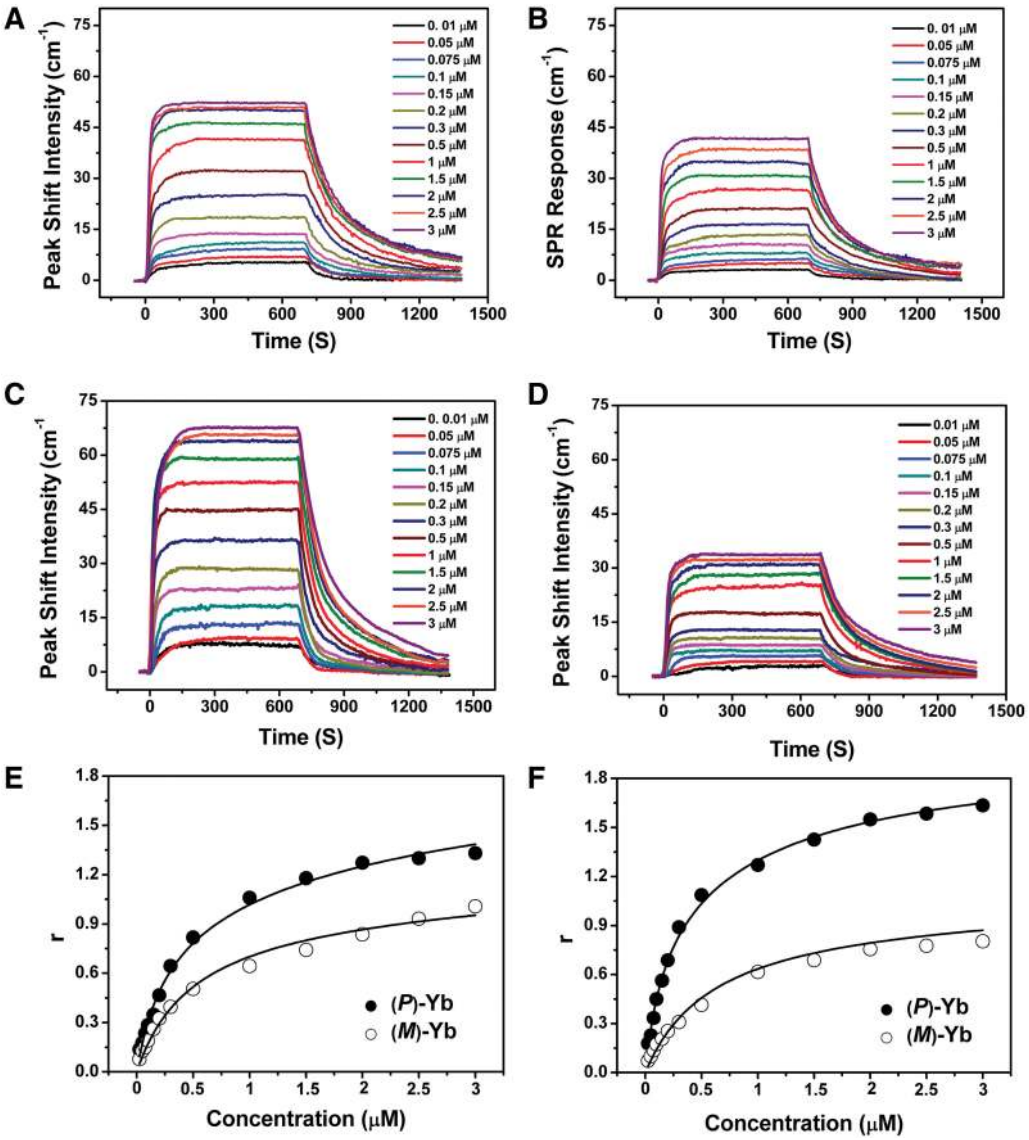

Figure 3. Up: SPR sensorgrams for the interactions of (*P*)-Yb (**A**) and (*M*)-Yb (**B**) with AT-DNA. Middle: SPR sensorgrams for the interactions of (*P*)-Yb (**C**) and (*M*)-Yb (**D**) with GC-DNA. DNA sequences are given in 'Materials and Methods' section. The concentrations of complexes are listed in the figure. Bottom: The binding curves of AT-DNA (**E**) and GC-DNA (**F**) binding with (*P*)-Yb (solid circles) and (*M*)-Yb (open circles). The data were fitted in a two-site model.

Table 2. M- and P-enantiomer DNA binding constants determined by SPR[a] and CD titration assays

	(*M*)-Yb			(*P*)-Yb		
	K_a^{SPR} (M^{-1})	K_a^{CD} (M^{-1})	$r_{complex/DNA}$	K_a^{SPR} (M^{-1})	K_a^{CD} (M^{-1})	$r_{complex/DNA}$
$(AT)_{17}$	K_1 2.1×10^6 K_2 0.3×10^5	2.5×10^5	1:4	K_1 4.1×10^6 K_2 2.6×10^5	5.4×10^5	1:4
$(GC)_{17}$	K_1 1.4×10^6 K_2 0.1×10^5	1.3×10^5	1:3	K_1 6.9×10^6 K_2 6.7×10^5	1.2×10^6	1:3

[a]The SDs were within 15% under the experimental conditions. K_a^{SPR} was obtained from the SPR assays. K_a^{CD} was estimated from the CD titritions and the details were described in 'Materials and Methods' section. The binding ratios ($r_{complex/DNA}$) were measured by CD titrations.

results from SPR assay. These results further supported that the enantiomers selectively binded to AT- and GC-DNA, which were in line with UV melting data and CD results. Moreover, these results demonstrate that P-enantiomer has GC preference over AT-DNA while M-enantiomer shows slightly AT preference. Such a binding preference for M-enantiomer and its opposite contribution to the thermal stability of GC-DNA and

AT-DNA can be used to explain that M-enantiomer initially stabilizes calf thymus DNA (ct-DNA, which consists of 42% GC and 58% AT) and then even destabilizes ct-DNA (Figure 1A). First, at low concentration of M-enantiomer, ct-DNA is excess, M-enantiomer would occupy its preferred AT binding sites that results in increasing DNA stability (39). With addition of more M-enantiomer, after occupied the preferred AT binding sites, M-enantiomer bind to GC binding sites and then destabilize DNA.

Possible DNA-binding mode

Since the chiral lanthanide complexes have large size and unique $4f^n$ electronic configuration and possess strong effects on NMR line broadening and chemical shifts (26), these made molecular dynamics simulation and NMR studies unsuccessful for exploring their DNA binding mode. The binding mode of the two enantiomers bound to DNA was further studied by the commonly used competitive binding assay using fluorescence and CD spectroscopy (38,53,54). It is well known that EB can intercalate into DNA through minor groove and Hoechst 33 258 is a classical DNA minor groove binder (28,38,40). When bound to DNA, their fluorescence is greatly enhanced. With this in mind, if the enantiomer competitively binds to the same sites of DNA as EB or Hoechst 33 258, the fluorescence of EB or Hoechst 33 258 would decrease because enantiomer binding to DNA should exclude EB or Hoechst 33 258 out of their binding sites. As shown in Figure 4A, EB fluorescence dramatically decreased when titrated ct-DNA with both M- and P-enantiomer, showing that the two enantiomers can exclude EB out of DNA minor groove (38,53,54), suggesting that the two enantiomers might bind to DNA minor groove. This was further supported by Hoechst 33 258 displacement (Figure 4B). Hoechst 33 258 fluorescence dramatically decreased upon the addition of both M- and P-enantiomer, indicating its displacement by the enantiomer from DNA minor groove, the same as EB displacement. In consideration of the large size of the macrocyclic chiral complex, the two enantiomers can be minor groove binders. To further identify this assumption, another competitive binding assay was carried out. MG is a proven DNA major groove binder (38,55). When MG bound to DNA, four induced CD signals characteristic of bound MG ~310, 430, 620 and 650 nm were observed (Figure 5). If the two enantiomers bind to DNA major groove, they would exclude MG out of DNA major groove and weaken the CD signals induced by MG. In fact, the induced CD signals are hardly influenced with addition of both the two enantiomers, which suggests that the two enantiomers do not competitively bind to DNA major groove (38,55). Although the induced CD signals of MG are not influenced, intriguingly, the CD band of DNA at 260 nm is increased significantly, that can be caused by the enantiomer binding. These results demonstrate that the two enantiomers do bind to DNA, but not bind in the major groove, further supporting that EB and Hoechst 33 258 fluorescence competitive data that the enantiomers bind to DNA minor groove. Thus, in

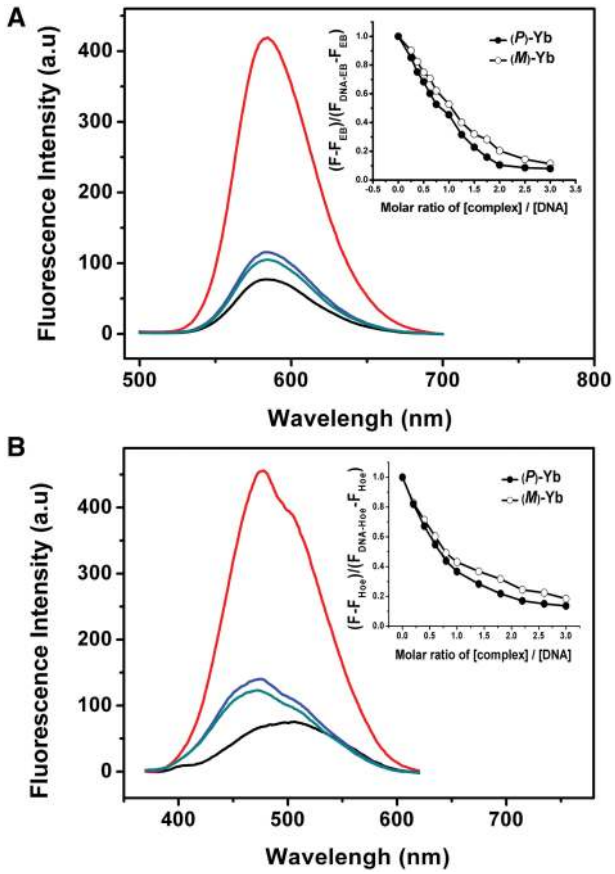

Figure 4. (**A**) Fluorescence emission spectra of EB alone (black); ct-DNA-EB (red); ct-DNA-EB after addition of (*P*)-Yb (green) and (*M*)-Yb (blue). (**B**) Fluorescence emission spectra of Hoechst 33258 alone (black); ct-DNA-Hoechst 33258 (red); ct-DNA-Hoechst 33258 after addition of (*P*)-Yb (green) and (*M*)-Yb (blue). Insert: Degree of fluorophore (EB, Hoechst 33 258) displacement with increased molar ratios of (*P*)-Yb to DNA (solid circles) and (*M*)-Yb to DNA (open circles). DNA was 20 μM in bp. EB and Hoechst 33 258 was 6.6 μM. The experiments were carried out in 5 mM Tris–HCl buffer (pH = 7.2) at 25°C.

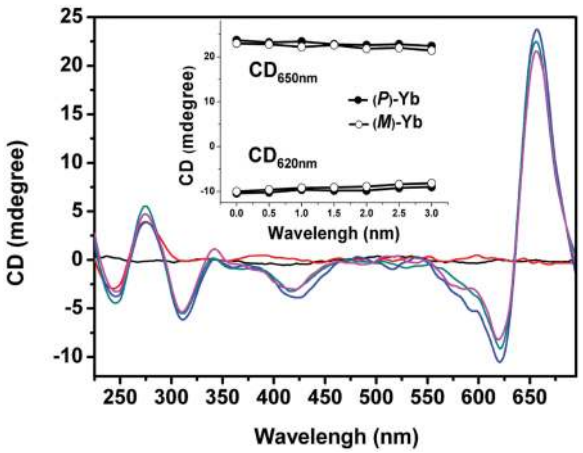

Figure 5. CD spectra of methylene green (black); ct-DNA (red); ct-DNA-methylene green (blue); ct-DNA-methylene green after addition of (*P*)-Yb (green) and (*M*)-Yb (pink). Insert: The change in ellipticity at 650 and 620 nm with increased molar ratios of (*P*)-Yb to DNA (solid circles) and (*M*)-Yb to DNA (open circles). DNA was 30 μM in bp. The experiments were carried out in 5 mM Tris–HCl buffer (pH = 7.2) at 25°C.

combination with UV melting and CD data, and EB, Hoechst 33 258 and MG competitive binding results, the two enantiomers can bind to DNA minor groove but not the major groove, further detailed studies are demanding for understanding their DNA binding mechanism.

Different effects on B-form duplex DNA and non-B-form DNA

Another intriguing feature of these two enantiomers is their ability in discriminating B-form duplex DNA among non-B form duplex DNA and quadruplex DNA. It is well known that GC-DNA and AT-DNA are in B-form, whereas polydApolydT which has distinct structural and functional properties and adopts a non-B-form conformation (27,38). As shown by the ΔT_m values in Table 3, unlike the two enantiomers binding to GC-DNA and AT-DNA, the two enantiomers hardly change the stability of polydApolydT, suggesting that they bound hardly to non-B-form polydApolydT. We also studied the binding of the enantiomers with anther two famous DNA structures, A-form and Z-form DNA (56,57). The results were showed in Supplementary Figures S7 and S8. Clearly, both of the two enantiomers hardly affected the structure and stability of A-form and Z-form DNA, indicating their weakly binding to these two DNA structures. These results further indicate that the two enantiomers are selectively binding to B-form DNA. To gain further insight into their selectivity on different DNA conformation, we also studied the interactions of these chiral complexes with different typical quadruplex DNA (7–9,58,59). Table 3 summarizes the melting data of typical G-quadruplex DNA and i-motif DNA upon the two enantiomers binding. Clearly, both M-enantiomer and P-enantiomer slightly influence G-quadruplex or i-motif DNA stability (7), indicating the enantiomer has B-form DNA preference. Considering that ionic strength may influence the selective binding of the complexes to G-quadruplex DNA and duplex DNA, we also studied the interactions of the enantiomers with G-quadruplex DNA and duplex DNA in physiological salt concentration (100 mM NaCl, pH = 7.2) and the results were shown in Supplementary Figure S9. Evidently, the enantiomers stabilized duplex ct-DNA and had no effect on G-quadruplex DNA (AG_3), indicating their selective binding to B-form DNA in physiological salt concentration. It should be pointed out that the degree of stabilization for ct-DNA was lower in higher ionic strength buffer than that in low ionic strength buffer. This indicates that electrostatic effect is playing an important role for the two enantiomers binding to duplex DNA due to their three positive charges. In combination of the above results, we expect that the two enantiomers can be potential structural probes for B-form DNA.

Table 3. Comparison of the effects of M- and P-enantiomer binding on the stability of different DNA

DNA	Structure	DNA T_m (°C)	DNA + M ΔT_m (°C)	DNA + P ΔT_m (°C)
ct-DNA	Duplex[a]	52.1	11.5	32.8
$(AT)_{17}$	Duplex[a]	35.7	11.8	26.7
$(GC)_{17}$	Duplex[a]	74.4	−12.3	15.5
$A_{22}T_{22}$	Duplex[a]	34.5	1.1	1.6
AG_3 in Na^+	Quadruplex[b]	53.1	−1.0	0
AG_3 in K^+	Quadruplex[c]	71.4	−0.9	−1.2
c-kit	Quadruplex[c]	67.0	0	0
c-myc	Quadruplex[c]	75.2	1.0	0
i-motif	Quadruplex[d]	43.1	0	−1.1

[a]In 5 mM Tris, pH = 7.2 buffer.
[b]In 5 mM Tris, 100 mM NaCl, pH = 7.2 buffer.
[c]In 5 mM Tris, 100 mM KCl, pH = 7.2 buffer.
[d]In 5 mM Tris buffer, pH = 5.5. DNA concentration was 20 μM in bp for duplex and 1 μM in strand for quadruplex.

CONCLUSION

Ligand–DNA interactions have numerous applications, such as in drug design, engineered gene regulation and DNA nanotechnology. Design and synthesis of metal complexes which selectively target specific genes or particular DNA structures have made significant progress in cancer chemotherapy. Here, we report that a pair of chiral helical macrocyclic lanthanide (III) complexes, (*M*)-Yb$[L_{ssssss}]^{3+}$ and (*P*)-Yb$[L_{RRRRRR}]^{3+}$, can enantioselectively bind to B-form DNA and show remarkably contrasting effects on GC-rich and AT-rich DNA. Neither of them can influence non-B-form DNA, nor G-quadruplex or i-motif DNA stability. P-enantiomer stabilizes both poly(dG-dC)$_2$ and poly(dA-dT)$_2$ while M-enantiomer stabilizes poly(dA-dT)$_2$, but destabilizes poly(dG-dC)$_2$. To our knowledge, this is the best example of chiral metal compounds to show such contrasting GC and AT preference. Ligand selectively stabilizing or destabilizing DNA can interrupt DNA–enzyme interactions and potentially affect DNA replication, transcription and repair. Therefore, the chiral compounds reported here may provide new insights into design of novel enantiomers targeting specific DNA with both sequence and conformation preference.

SUPPLEMENTARY DATA

Supplementary Data are available at NAR Online: Supplementary Figures 1–9.

FUNDING

The National Basic Research Program of China [2011CB936004, 2012CB720602]; National Natural Science Foundation of China [20831003, 90813001, 20833006, 90913007, 20903086]. Funding for open access charge: The National Basic Research Program of China; National Natural Science Foundation of China.

Conflict of interest statement. None declared.

REFERENCES

1. Barton,J.K. (1986) Metals and DNA: molecular left-handed complements. *Science*, **233**, 727–734.
2. Fuertes,M.A., Cepeda,V., Alonso,C. and Perez,J.M. (2006) Molecular mechanisms for the B-Z transition in the example of

poly d(G-C)center dot d(G-C) polymers. *A critical review*. *Chem. Rev*., **106**, 2045–2064.
3. Muller,B.C., Raphael,A.L. and Barton,J.K. (1987) Evidence for altered DNA conformations in the simian virus 40 genome: site-specific DNA cleavage by the chiral complex Λ-tris(4,7-diphenyl-1, 10-phenanthroline)cobalt(III). *Proc. Natl Acad. Sci. USA*, **84**, 1764–1768.
4. Barton,J.K., Basile,L.A., Danishefsky,A. and Alexandrescu,A. (1984) Chiral probes for the handedness of DNA helices: enantiomers of tris(4, 7-diphenylphenanthroline)ruthenium(II). *Proc. Natl Acad. Sci. USA*, **81**, 1961–1965.
5. Qu,X., Trent,J.O., Fokt,I., Priebe,W. and Chaires,J.B. (2000) Allosteric, chiral-selective drug binding to DNA. *Proc. Natl Acad. Sci. USA*, **97**, 12032–12037.
6. Xu,Y., Zhang,Y.X., Sugiyama,H., Umano,T., Osuga,H. and Tanaka,K. (2004) (P)-Helicene displays chiral selection in binding to Z-DNA. *J. Am. Chem. Soc*., **126**, 6566–6567.
7. Yu,H.J., Wang,X.H., Fu,M.L., Ren,J. and Qu,X. (2008) Chiral metallo-supramolecular complexes selectively recognize human telomeric G-quadruplex DNA. *Nucleic Acids Res*., **36**, 5695–5703.
8. Yu,H., Zhao,C., Chen,Y., Fu,M., Ren,J. and Qu,X. (2009) DNA loop sequence as the determinant for chiral supramolecular compound G-quadruplex selectivity. *J. Med. Chem*., **53**, 492–498.
9. Zhao,C., Geng,J., Feng,L., Ren,J. and Qu,X. (2011) Chiral metallo–supramolecular complexes selectively induce human telomeric G-quadruplex formation under salt-deficient conditions. *Chem. Eur. J*., **17**, 8209–8215.
10. Shinohara,K., Sannohe,Y., Kaieda,S., Tanaka,K., Osuga,H., Tahara,H., Xu,Y., Kawase,T., Bando,T. and Sugiyama,H. (2010) A chiral wedge molecule inhibits telomerase activity. *J. Am. Chem. Soc*., **132**, 3778–3782.
11. Boger,D.L., Johnson,D.S. and Yun,W. (1994) (+)- and ent-(-)-Duocarmycin SA and (+)- and ent-(-)-N-BOC-DSA DNA alkylation properties.alkylation site models that accommodate the offset AT-rich adenine N3 alkylation selectivity of the enantiomeric agents. *J. Am. Chem. Soc*., **116**, 1635–1656.
12. Tsukube,H. and Shinoda,S. (2002) Lanthanide complexes in molecular recognition and chirality sensing of biological substrates. *Chem. Rev*., **102**, 2389–2403.
13. Song,G. and Ren,J. (2010) Recognition and regulation of unique nucleic acid structures by small molecules. *Chem. Commun*., **46**, 7283–7294.
14. Georgiades,S.N., Abd Karim,N.H., Suntharalingam,K. and Vilar,R. (2010) Interaction of metal complexes with G-quadruplex DNA. *Angew. Chem. Int. Ed*., **49**, 4020–4034.
15. Önfelt,B., Lincoln,P. and Nordén,B. (2001) Enantioselective DNA threading dynamics by phenazine-linked $[Ru(phen)_2dppz]^{2+}$ dimers. *J. Am. Chem. Soc*., **123**, 3630–3637.
16. Boerner,L.J.K. and Zaleski,J.M. (2005) Metal complex-DNA interactions: from transcription inhibition to photoactivated cleavage. *Curr. Opin. Chem. Biol*., **9**, 135–144.
17. Erkkila,K.E., Odom,D.T. and Barton,J.K. (1999) Recognition and reaction of metallointercalators with DNA. *Chem. Rev*., **99**, 2777–2795.
18. Zeglis,B.M., Pierre,V.C. and Barton,J.K. (2007) Metallo-intercalators and metallo-insertors. *Chem. Commun*., 4565–4579.
19. Liu,H.-K. and Sadler,P.J. (2011) Metal complexes as DNA intercalators. *Acc. Chem. Res*., **44**, 349–359.
20. Barry,N.P.E., Abd Karim,N.H., Vilar,R. and Therrien,B. (2009) Interactions of ruthenium coordination cubes with DNA. *Dalton Trans*., 10717–10719.
21. Oleksi,A., Blanco,A.G., Boer,R., Usón,I., Aymamí,J., Rodger,A., Hannon,M.J. and Coll,M. (2006) Molecular recognition of a three-way DNA junction by a metallosupramolecular helicate. *Angew. Chem. Int. Ed*., **45**, 1227–1231.
22. Louie,A.Y., Huber,M.M., Ahrens,E.T., Rothbacher,U., Moats,R., Jacobs,R.E., Fraser,S.E. and Meade,T.J. (2000) In vivo visualization of gene expression using magnetic resonance imaging. *Nat. Biotechnol*., **18**, 321–325.
23. Caravan,P., Ellison,J., McMurry,T. and Lauffer,R. (1999) Gadolinium(III) chelates as MRI contrast agents: structure, dynamics, and applications. *Chem. Rev*., **99**, 2293–2352.
24. Franklin,S.J. (2001) Lanthanide-mediated DNA hydrolysis. *Curr. Opin. Chem. Biol*., **5**, 201–208.
25. Branum,M.E. and Que,L. Jr (1999) Double-strand DNA hydrolysis by dilanthanide complexes. *J. Biol. Inorg. Chem*., **4**, 593–600.
26. Zhang,H.Y., Yu,H.J., Ren,J. and Qu,X. (2006) PolydA and polyrA self-structured by a europium and amino acid complex. *FEBS Lett*., **580**, 3726–3730.
27. Zhang,H.Y., Yu,H.J., Ren,J. and Qu,X. (2006) Reversible B/Z-DNA transition under the low salt condition and non-B-form polydApolydT selectivity by a cubane-like europium-L-aspartic acid complex. *Biophysical J*., **90**, 3203–3207.
28. Geng,J., Zhao,C.Q., Ren,J.S. and Qu,X.G. (2010) Alzheimer's disease amyloid beta converting left-handed Z-DNA back to right-handed B-form. *Chem.Comm*., **46**, 7187–7189.
29. Bueren-Calabuig,J.A., Giraudon,C., Galmarini,C.M., Egly,J.M. and Gago,F. (2011) Temperature-induced melting of double-stranded DNA in the absence and presence of covalently bonded antitumour drugs: insight from molecular dynamics simulations. *Nucleic Acids Res*., **39**, 8248–8257.
30. Hofr,C. and Brabec,V. (2001) Thermal and thermodynamic properties of duplex DNA containing site-specific interstrand cross-link of antitumor cisplatin or its clinically ineffective trans isomer. *J. Biol. Chem*., **276**, 9655–9661.
31. Negri,A., Marco,E., García-Hernández,V., Domingo,A., Llamas-Saiz,A.L., Porto-Sandá,S., Riguera,R., Laine,W., David-Cordonnier,M.-H., Bailly,C. *et al*. (2007) Antitumor activity, X-ray crystal structure, and DNA binding properties of thiocoraline A, a natural bisintercalating thiodepsipeptide. *J. Med. Chem*., **50**, 3322–3333.
32. Lenglet,G. and David-Cordonnier,M.-H. (2010) DNA-destabilizing agents as an alternative approach for targeting DNA: mechanisms of action and cellular consequences. *J. Nucleic Acids*, **2010**, 290935.
33. Yang,W. (2008) Structure and mechanism for DNA lesion recognition. *Cell Res*., **18**, 184–197.
34. Huang,J.C., Zamble,D.B., Reardon,J.T., Lippard,S.J. and Sancar,A. (1994) HMG-domain proteins specifically inhibit the repair of the major DNA adduct of the anticancer drug cisplatin by human excision nuclease. *Proc. Natl Acad. Sci. USA*, **91**, 10394–10398.
35. Mudasir., Yoshioka,N. and Inoue,H. (2008) Enantioselective DNA binding of iron(II) complexes of methyl-substituted phenanthroline. *J. Inorg. Biochem*., **102**, 1638–1643.
36. Sun,D., Liu,Y., Liu,D., Zhang,R., Yang,X. and Liu,J. (2012) Stabilization of G-quadruplex DNA, inhibition of telomerase activity and live cell imaging studies of chiral ruthenium (II) complexes. *Chem. Eur. J*., **18**, 4285–4295.
37. Chaires,J.B. (1998) Drug-DNA interactions. *Curr. Opin. Struct. Biol*., **8**, 314–320.
38. Li,X., Peng,Y.H. and Qu,X.G. (2006) Carbon nanotubes selective destabilization of duplex and triplex DNA and inducing B-A transition in solution. *Nucleic Acids Res*., **34**, 3670–3676.
39. Qu,X., Ren,J., Riccelli,P., Benight,A.S. and Chaires,J.B. (2003) Enthalpy/entropy compensation: influence of DNA flanking sequence on the binding of 7-amino actinomycin D to its primary binding site in short DNA duplexes. *Biochemistry*, **42**, 11960–11967.
40. Li,X., Peng,Y., Ren,J. and Qu,X. (2006) Effect of DNA flanking sequence on charge transport in short DNA duplexes. *Biochemistry*, **45**, 13543–11550.
41. Gregoliński,J. and Lisowski,J. (2006) Helicity inversion in lanthanide(III) complexes with chiral nonaaza macrocyclic ligands. *Angew. Chem. Int. Ed*., **45**, 6122–6126.
42. Gregoliński,J., Starynowicz,P., Hua,K.T., Lunkley,J.L., Muller,G. and Lisowski,J. (2008) Helical lanthanide(III) complexes with chiral nonaaza macrocycle. *J. Am. Chem. Soc*., **130**, 17761–17773.
43. Li,X., Peng,Y.H., Ren,J. and Qu,X. (2006) Carboxyl-modified single-walled carbon nanotubes selectively induce human telomeric i-motif formation. *Proc. Natl Acad. Sci. USA*, **103**, 19658–19663.
44. Amemiya,R. and Yamaguchi,M. (2008) Chiral recognition in noncovalent bonding interactions between helicenes: right-handed helix favors right-handed helix over left-handed helix. *Org. Biomol. Chem*., **6**, 26–35.

45. Miyoshi,D., Karimata,H. and Sugimoto,N. (2006) Hydration regulates thermodynamics of G-quadruplex formation under molecular crowding conditions. *J. Am. Chem. Soc.*, **128**, 7957–7963.
46. Mergny,J.L. and Lacroix,L. (2003) Analysis of thermal melting curves. *Oligonucleotides*, **13**, 515–537.
47. Rodger,A., Blagbrough,I.S., Adlam,G. and Carpenter,M.L. (1994) DNA binding of a spermine derivative: spectroscopic study of anthracene-9-carbonyl-n1-spermine with poly[d(G-C)•(d(G-C))] and poly[d(A-T) • d(A-T)]. *Biopolymers*, **34**, 1583–1593.
48. Neidle,S. (2001) DNA minor-groove recognition by small molecules. *Nat. Prod. Rep.*, **18**, 291–309.
49. Lin,L.-P., Huang,L.-S., Lin,C.-W., Lee,C.-K., Chen,J.-L., Hsu,S.-M. and Lin,S. (2005) Determination of binding constant of DNA-binding drug to target DNA by surface plasmon resonance biosensor technology. *Curr. Drug Targets*, **5**, 61–72.
50. Liu,Y., Chai,Y., Kumar,A., Tidwell,R.R., Boykin,D.W. and Wilson,W.D. (2012) Designed compounds for recognition of 10 base pairs of DNA with two AT binding sites. *J. Am. Chem. Soc.*, **134**, 5290–5299.
51. González-Bulnes,L. and Gallego,J. (2009) Indirect effects modulating the interaction between DNA and a cytotoxic bisnaphthalimide reveal a two-step binding process. *J. Am. Chem. Soc.*, **131**, 7781–7791.
52. Jecklin,M.C., Schauer,S., Dumelin,C.E. and Zenobi,R. (2009) Label-free determination of protein–ligand binding constants using mass spectrometry and validation using surface plasmon resonance and isothermal titration calorimetry. *J. Mol. Recognit.*, **22**, 319–329.
53. Monchaud,D., Allain,C., Bertrand,H., Smargiasso,N., Rosu,F., Gabelica,V., De Cian,A., Mergny,J.L. and Teulade-Fichou,M.P. (2008) Ligands playing musical chairs with G-quadruplex DNA: a rapid and simple displacement assay for identifying selective G-quadruplex binders. *Biochimie*, **90**, 1207–1223.
54. Boger,D.L., Fink,B.E., Brunette,S.R., Tse,W.C. and Hedrick,M.P. (2001) A simple, high-resolution method for establishing DNA binding affinity and sequence selectivity. *J. Am. Chem. Soc.*, **123**, 5878–5891.
55. Tuite,E., Sehlstedt,U., Hagmar,P., Nordén,B. and Takahashi,M. (1997) Effects of minor and major groove-binding drugs and intercalators on the DNA association of minor groove-binding proteins RecA and deoxyribonuclease I detected by flow linear dichroism. *Eur. J. Bichem.*, **243**, 482–492.
56. Narainui,H., Akutsu,H. and Kyogoku,Y. (1985) Alcohol induced B-A transition of DNAs with different base compositions studied by circular dichroism. *J. Biochem.*, **98**, 629–636.
57. Zacharias,W., Larson,J.E., Klysik,J., Stirdivant,S.M. and Wells,R.D. (1982) Conditions which cause the right-handed to left-handed DNA conformational transitions. *J. Biochem.*, **257**, 2775–2782.
58. Reed,J.E., Arnal,A.A., Neidle,S. and Vilar,R. (2006) Stabilization of G-quadruplex DNA and inhibition of telomerase activity by square-planar nickel(II) complexes. *J. Am. Chem. Soc.*, **128**, 5992–5993.
59. Shirude,P.S., Gillies,E.R., Ladame,S., Godde,F., Shin-ya,K., Huc,I. and Balasubramanian,S. (2007) Macrocyclic and helical oligoamides as a new class of G-quadruplex ligands. *J. Am. Chem. Soc.*, **129**, 11890–11891.